

Children's Mercy Kansas City

SHARE @ Children's Mercy

Manuscripts, Articles, Book Chapters and Other Papers

1-24-2020

Infection-induced signals generated at the plasma membrane epigenetically regulate Wnt signaling in vitro and in vivo

Ishfaq Ahmed

Badal Chandra Roy

Laxmi Uma Maheswar Rao Jakkula

Dharmalingam Subramaniam

Prasad Dandawate

See next page for additional authors

Let us know how access to this publication benefits you

Follow this and additional works at: <https://scholarlyexchange.childrensmercy.org/papers>

Recommended Citation

Ahmed I, Roy BC, Rao Jakkula LUM, et al. Infection-induced signals generated at the plasma membrane epigenetically regulate Wnt signaling in vitro and in vivo. J Biol Chem. 2020;295(4):1021-1035. doi:10.1074/jbc.RA119.010285

This Article is brought to you for free and open access by SHARE @ Children's Mercy. It has been accepted for inclusion in Manuscripts, Articles, Book Chapters and Other Papers by an authorized administrator of SHARE @ Children's Mercy. For more information, please contact hlsteel@cmh.edu.

Creator(s)

Ishfaq Ahmed, Badal Chandra Roy, Laxmi Uma Maheswar Rao Jakkula, Dharmalingam Subramaniam, Prasad Dandawate, Shrikant Anant, Venkatesh Sampath, and Shahid Umar

Infection-induced signals generated at the plasma membrane epigenetically regulate Wnt signaling *in vitro* and *in vivo*

Received for publication, July 20, 2019, and in revised form, December 5, 2019. Published, Papers in Press, December 13, 2019, DOI 10.1074/jbc.RA119.010285

Ishfaq Ahmed^{‡1}, Badal Chandra Roy^{‡1}, Laxmi Uma Maheswar Rao Jakkula[‡],  Dharmalingam Subramaniam[§],  Prasad Dandawate[§], Shrikant Anant[§], Venkatesh Sampath[¶], and Shahid Umar^{‡2}

From the Departments of [‡]Surgery and [§]Cancer Biology, University of Kansas Medical Center, Kansas City, Kansas 66160 and the [¶]Division of Neonatology, Children's Mercy Hospital, Kansas City, Missouri 64108

Edited by Alex Tokar

Wnt signaling regulates immunomodulatory functions during infection and inflammation. Employing NCCIT and HCT116 cells, having high endogenous Wnt signaling, we observed elevated levels of low-density lipoprotein receptor-related protein 5/6 (LRP5/6) and Frizzled class receptor 10 (FZD10) and increases in β -catenin, doublecortin-like kinase 1 (DCLK1), CD44 molecule (CD44), and aldehyde dehydrogenase 1 family member A1 (ALDH1A1). siRNA-induced knockdown of these receptors antagonized TOPflash reporter activity and spheroid growth *in vitro* and elevated Wnt-inhibitory factor 1 (WIF1) activity. Elevated mRNA and protein levels of LRP5/6 and FZD10 paralleled expression of WNT2b and WNT4 in colonic crypts at days 6 and 12 post-infection with *Citrobacter rodentium* (CR) and tended to decline at days 20–34. The CR mutant *escV* or the tankyrase inhibitor XAV939 attenuated these responses. A three-dimensional organoid assay in colonic crypts isolated from CR-infected mice revealed elevated levels of LRP5/6 and FZD10 and β -catenin co-localization with enhancer of zeste 2 polycomb repressive complex 2 subunit (EZH2). Co-immunoprecipitation in the membrane fraction revealed that axin associates with LRP5/6 in CR-infected crypts, and this association was correlated with increased β -catenin. Colon tumors from either CR-infected *Apc*^{Min/+} or azoxymethane/dextran sodium sulfate (AOM/DSS)-treated mice had high LRP5/6 or FZD10 levels, and chronic Notch blockade through the γ -secretase inhibitor dibenzazepine down-regulated LRP5/6 and FZD10 expression. In CR-responsive CT-26 cells, siRNA-induced LRP5/6 or FZD10 knockdown antagonized TOPflash reporter activity. Elevated miR-153-3p levels correlated with LRP5/6 and FZD10, and miR-153-3p sequestration via a plasmid-based miR inhibitor system attenuated Wnt signaling. We conclude that infection-induced signals from the plasma membrane epigenetically regulate Wnt signaling.

Signaling via the Wnt pathway controls myriad biological phenomena during development and throughout adult life. Aberrant Wnt signaling, however, underlies a wide range of pathologies, including colorectal cancer (CRC)³ in humans (1, 2). In unstimulated cells, cytosolic β -catenin associated with axin and APC undergoes phosphorylation and degradation by the ubiquitin/proteasomal pathway. Wnt signaling is initiated at the cell surface when Wnt proteins bind to co-receptors LRP5/6 and FZD, in which *de novo* synthesized β -catenin escapes degradation and acts as a transcriptional co-activator in association with T cell factor-4 (TCF-4) (3).

In CRC, the majority of Wnt pathway mutations occur in the gene encoding β -catenin (CTNNB1) (4). However, aberrant activation of the Wnt pathway can also be driven by inactivating mutations in zinc and RING finger 3 (ZNF3) and RING finger protein 43 (RNF43), which encodes tumor suppressor E3 ubiquitin ligases (5). These mutations are frequently present in CRC and endometrial cancers, leading to stabilization and higher levels of FZD receptors (5, 6), which underscores a role for upstream Wnt signaling in these tumors. Similarly, mutant mice homozygous for LRP6 show embryonic defects and die at birth, whereas *Lrp5*-deficient mice are viable, although with a low-bone-mass phenotype (7–9). In humans, LRP6 variants have been identified in individuals with an early-onset CRC (≤ 30 years of age) and contribute toward heterogeneous susceptibility to CRC (9). Despite these advances, a systematic study looking beyond mutational activation of Wnt signaling through signals generated at the plasma membrane in a non-neoplastic colonic epithelium is lacking.

Cancer stem cells (CSCs), a heterogeneous population of cells with overlapping and sometimes unique combinations of markers such as aldehyde dehydrogenase-1A1 (ALDH1A1), Dclk1, CD133, and Lgr5, have well-documented associations with normal stem cells, cancer, CSCs, and chemoresistance.

This work was supported by National Institutes of Health Grants R01CA185322 (to S.U.) and R01DK117296-01A1 (to V.S.). The authors declare that they have no conflicts of interest with the contents of this article. The content is solely the responsibility of the authors and does not necessarily represent the official views of the National Institutes of Health. This article contains Figs. S1–S5.

¹ Both authors contributed equally to this work.

² To whom correspondence should be addressed: Dept. of Surgery, University of Kansas Medical Center, 3901 Rainbow Blvd., 4028 Wahl Hall East, Kansas City, KS 66160. Tel.: 913-945-6337; Fax: 913-945-6327; E-mail: sumar@kumc.edu.

³ The abbreviations used are: CRC, colorectal cancer; AOM, azoxymethane; DSS, dextran sodium sulfate; CSC, cancer stem cell; miRNA, microRNA; CR, *Citrobacter rodentium*; ISH, *in situ* hybridization; CLP, crypt-denuded lamina propria; DBZ, dibenzazepine; 3D, three-dimensional; PCNA, proliferating cell nuclear antigen; APC, adenomatous polyposis coli; PMIS, plasmid-based miR inhibitor system; CK1 ϵ , casein kinase-1 ϵ ; LRP, low-density lipoprotein receptor-related protein; TCF, T cell factor; ANOVA, analysis of variance; qRT-PCR, quantitative RT-PCR; ERK, extracellular signal-regulated kinase; MEK, mitogen-activated protein kinase/extracellular signal-regulated kinase kinase.

This is an Open Access article under the [CC BY](https://creativecommons.org/licenses/by/4.0/) license.

Epigenetic regulation of Wnt signaling through enteric pathogen

Markers including CD44, Lgr5, Dclk1, and EpCAM are especially relevant in CRC (10–12), and down-regulation of Lgr5 expression, which coincides with reduced Wnt signaling, or diphtheria toxin–induced depletion of Dclk1 attenuates colon tumorigenesis (10, 13, 14). Despite their clinical relevance, the mechanism of CSC regulation is poorly understood.

MicroRNAs (miRNAs) are a class of small noncoding RNA molecules involved in the fine-tuning of fundamental biological processes such as proliferation, differentiation, survival, and apoptosis in many cell types. Recent evidence suggests that miRNAs also play a key role in regulating CSC function by modulating transcription factors and downstream signaling pathways activated in CSCs (15). We previously determined that miR-203 regulates expression of a Wnt antagonist WIF-1, in a nonneoplastic but hyperproliferating colonic epithelium in response to an enteric pathogen (16). How enteric pathogen-induced changes in the components of the Wnt pathway affect the stemness potential of these CSCs remains to be elucidated.

Human enteric pathogens such as enteropathogenic *Escherichia coli*, enterohemorrhagic *E. coli*, and the murine pathogen *Citrobacter rodentium* (CR), which uses attaching-and-effacing lesion formation as a major mechanism of tissue targeting and infection, represent the classic genome organization (17). Both EPEC and EHEC are poorly pathogenic in mice but infect humans and domestic animals. In contrast, CR is a natural mouse pathogen that is related to *E. coli* and provides an excellent *in vivo* model for attaching-and-effacing lesion-forming pathogens (18). CR also provides a model of infections that are mainly restricted to the lumen of the intestine. Work from our laboratory provided the initial evidence of CR's involvement in the activation of the Wnt signaling pathway (19). Published and ongoing studies in our laboratory have further demonstrated that CR-induced Wnt signaling does not work alone; rather, cross-talk with Notch and NF- κ B signaling pathways shapes the pathogenesis of CR-induced crypt hyperplasia (20, 21). Similar studies with *Salmonella* strains expressing AvrA have shown enhanced nuclear translocation and acetylation of β -catenin that lead to a significant increase in downstream targets (22). We add to this existing knowledge by further investigating the role of bacterial infection in initiating Wnt signaling at the plasma membrane and how this culminates in β -catenin–dependent colonic crypt hyperplasia. We hypothesized that signals generated at the plasma membrane in response to CR infection will involve both Frizzled and LRP5/6 receptors to epigenetically modify Wnt signaling. In the current study, we have attempted to systematically characterize the components of the Wnt signaling machinery using *in vitro* and *in vivo* approaches and, based on our findings, suggest that targeting individual markers of CSCs may not be sufficient to eradicate CSCs in an environment fueled by high Wnt signaling.

Results

We began our quest to systematically analyze the components of Wnt signaling by screening NCCIT and PA-1 teratocarcinoma cell lines. These cells endogenously express high levels of Wnt signaling components and therefore provide an excellent system in which to systematically knock down membrane receptors and examine how that impacts downstream

signaling and stemness. As depicted in Fig. 1 (Ai–Aiii), we detected varying levels of LRP5, LRP6, and Fzd10 in both NCCIT and PA-1 cell lines, respectively. At the protein level, NCCIT cells expressed these proteins at the highest levels compared with PA-1 cells. These results were comparable in the HCT116 colon cancer cell line. β -Catenin, either at the mRNA or protein level, also exhibited strong expression in the NCCIT cells (Fig. 1, Aiv and Bi). When we examined the protein levels of various markers of CSCs, both Dclk1 and CD44 levels were elevated in NCCIT and PA-1 cell lines, whereas increased levels of ALDH1A1 were recorded in both NCCIT and HCT116 cells, respectively (Fig. 1Biv). We next performed TOPflash and WIF-1 reporter assays following knockdown of both LRP5 and LRP6 in either HEK293 or NCCIT cells, respectively. As depicted in Fig. 1 (Ci and Cii), knocking down both LRP5 and LRP6 decreased TOPflash reporter activities albeit at varying levels. WIF-1 reporter activities, on the other hand, exhibited a slight increase following knockdown of these receptors (Fig. 1, Ciii and Civ). Fig. S1 represents the real-time PCR levels for LRP5, LRP6, and Fzd10 following their knockdown. Further investigation into the expression levels of Wnt antagonists revealed increases in DKK1, -2, and -3 as well as SFRP1 and -2 and WIF1, particularly in Fzd10-knocked down cells (Fig. S1). Encouraged by these results, we next performed spheroid assays in NCCIT cells as a measure of stem-cell functions (or stemness) (23). As depicted in Fig. 1 (Di and Dii), knockdown of both LRP5 and Fzd10 significantly reduced spheroid growth, whereas spheroid growth was less efficiently blocked following LRP6 knockdown. Because we showed previously (16) that EZH2 is an integral component of CSC gene repertoire, knockdown of EZH2 reproducibly blocked spheroid growth (Fig. 1Dii) that validated the efficiency of these assays.

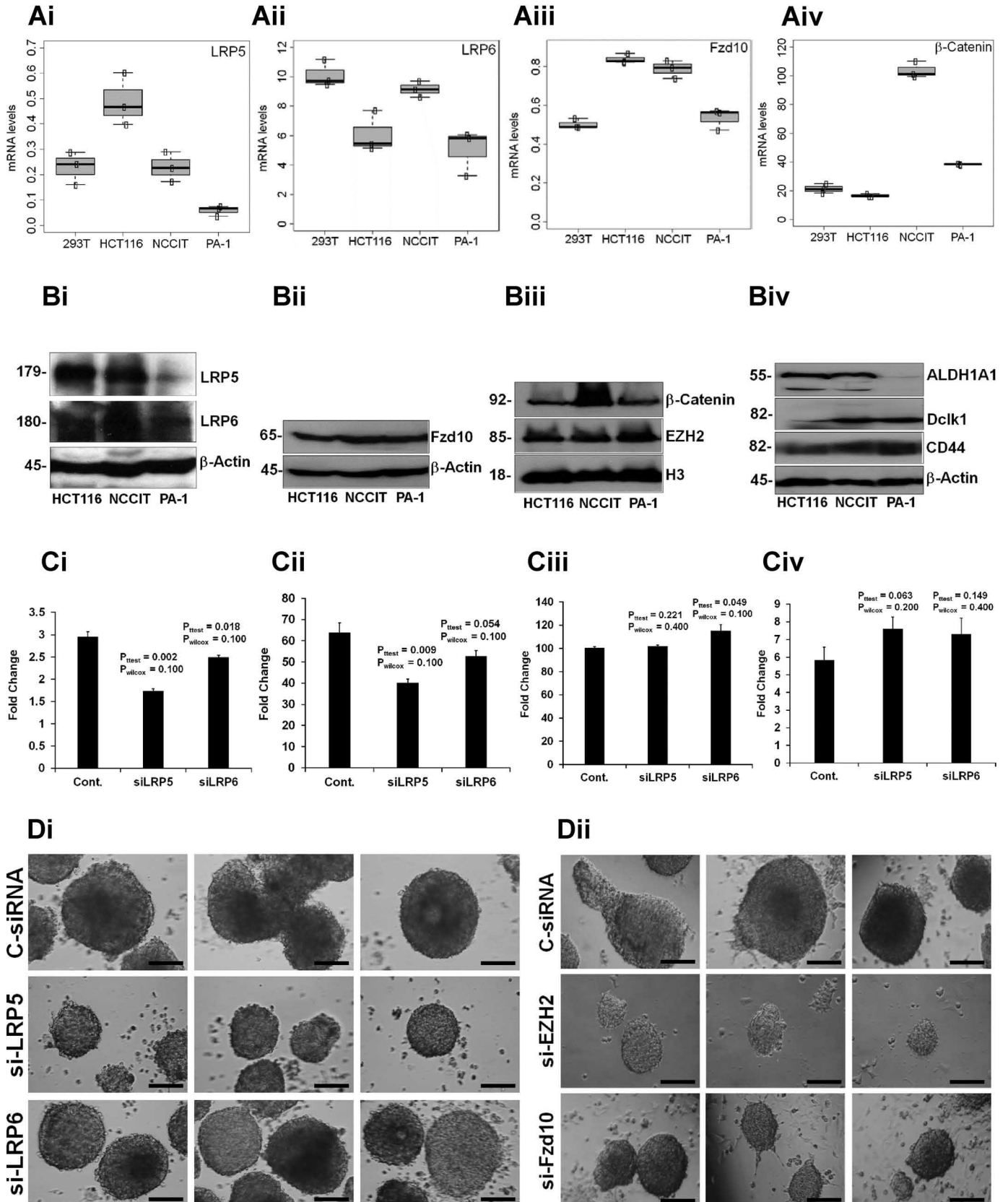
Based on these results, we next started focusing on murine models of colonic crypt hyperplasia and intestinal tumorigenesis to systematically analyze epithelial responses to CR infection and how it affected the expression of Wnt ligands and LRP5/6 and Fzd10 expression. As depicted in Fig. 2 (A and B), increases in LRP5, LRP6, and Fzd10 either at the mRNA level using *in situ* hybridization (ISH; Fig. 2A) or at the protein level (Fig. 2B) paralleled increases in Wnt2b and Wnt4 ligand expression in the crypts at days 6 and 12 post-CR infection (progression of hyperplasia) with a declining trend at days 20–34 (regression of hyperplasia) (Fig. 2Ci). Wnt2b and Wnt4 expression in the crypt-denuded lamina propria (CLP), on the other hand, was only noticeable during the regression phase of crypt hyperplasia (Fig. 2Cii). To functionally link Wnt2b to downstream Wnt signaling, RT-PCR in NCCIT cells transfected with siRNAs to Wnt2b showed a decline in Wnt2b expression coincident with decreases in TOPflash reporter activity (Fig. S2, A–C). Thus, CR infection induces significant changes in Wnt ligand and receptor expression that may explain its ability to modulate Wnt signaling that culminates in β -catenin–induced crypt hyperplasia (16, 19, 20).

In the context of intestinal homeostasis, there is evidence of significant cross-talk between the Wnt and the Notch pathways (20, 21). We have shown previously that CR infection regulates a functional cross-talk between these pathways and that chronic blockade of the Notch pathway also interferes with

Epigenetic regulation of Wnt signaling through enteric pathogen

Wnt signaling, leading to inflammation and colitis (20). To investigate whether the cross-talk also influenced the expression of Wnt receptors, we performed ISH, and intriguingly, the

Notch blocker dibenzazepine (DBZ) significantly inhibited expression of LRP5, LRP6, and Fzd10 compared with CR-infected alone (Fig. 3A). Follow-up Western blots revealed



Epigenetic regulation of Wnt signaling through enteric pathogen

decreases in relative levels of LRP5/6 and Fzd10 in CR + DBZ-treated crypt extracts compared with CR alone (Fig. 3B). Because pivotal aspects of tissue homeostasis are often deduced from studies of tumor cells, we next performed ISH on *Apc^{Min/+}* mice that develop tumors in the colon in response to CR infection (24, 25). As depicted in Fig. 4, CR infection led to significant increase in LRP5/6 and Fzd10 expression at 12 days post-infection compared with uninfected controls, similar to data shown in Figs. 2 and 3, whereas tumors resembling adenomas in the distal colons of these mice at 3 months of age also exhibited significant increase in the levels of these receptors. To further understand whether these changes were not unique to CR infection, we next examined AOM and AOM/DSS models of colon cancer. As depicted in Fig. 4, AOM treatment alone had significant effect on the expression of these receptors, whereas AOM/DSS tumors further revealed high LRP5/6 and Fzd10 immunoreactivity compared with adjacent controls (Fig. 4). These findings provide compelling evidence that supports the notion that infection induces up-regulation of Wnt components that underlie early stages of colon carcinogenesis.

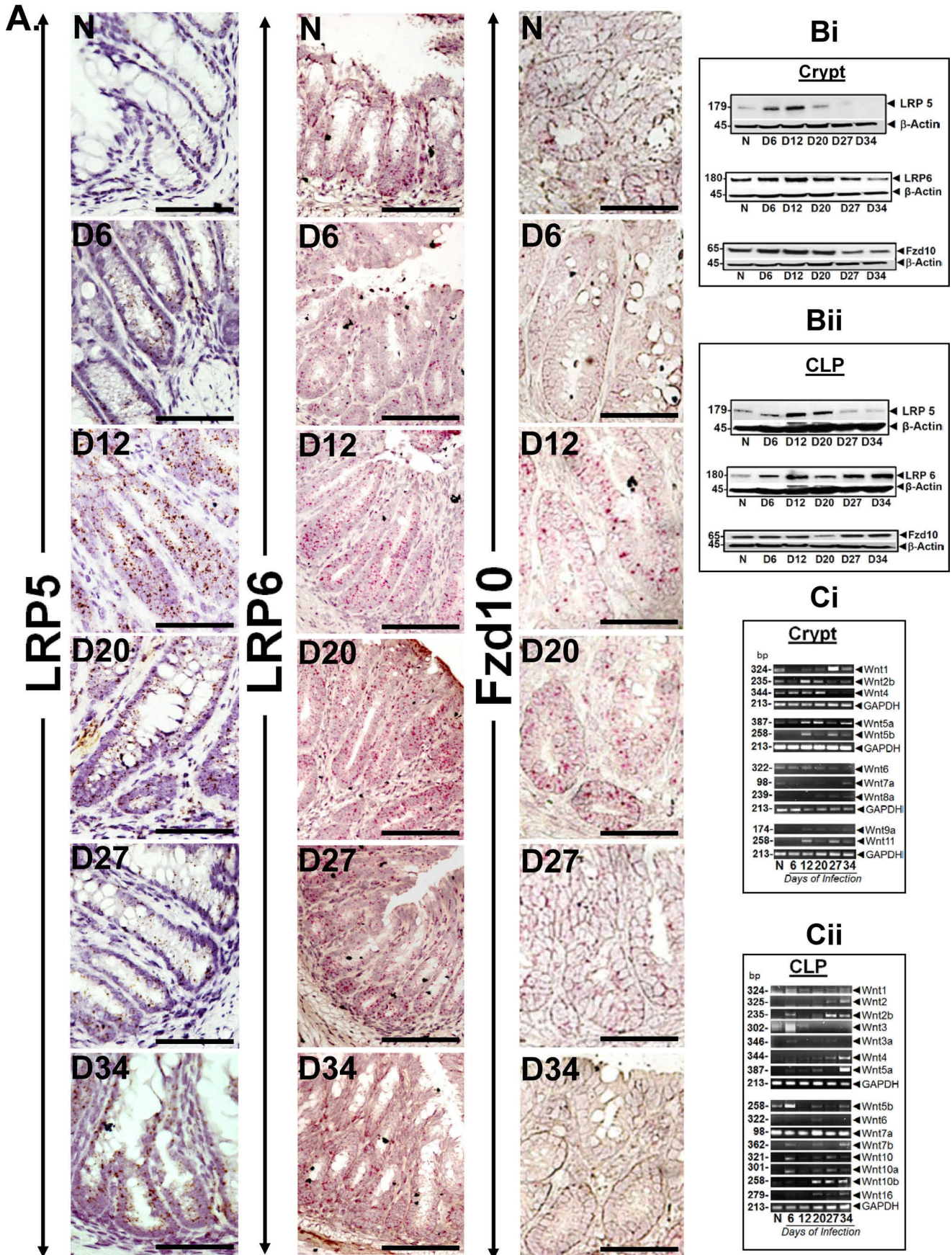
Mucosal surfaces lining the gastrointestinal tract possess a complex three-dimensional (3D) structure that facilitates tissue-specific functions. Because appropriate modeling of the 3D microenvironment is important for mimicking disease, which led to development and application of 3D organoid models (26), we next isolated intestinal and colonic crypts from uninfected or CR-infected mice and grew them as 3D organoids. These organoids were subsequently fixed and stained for LRP5/6 and Fzd10 as well as for *Lgr5* and *Dclk1*, respectively. As shown in Fig. 5, infection with CR, despite its being a colon pathogen, impacted both enteroid and colonoid growth along with measurable increases in LRP5/6, Fzd10, and *Lgr5* immunoreactivity. The extent of *Dclk1* staining, particularly in colonoids from CR-infected mice, on the other hand, was lower compared with uninfected controls, consistent with our previous report (27). To see how these changes impacted signaling components EZH2 and β -catenin, we next stained the colonoids for these downstream targets. As shown in Fig. 6A, colonoids from CR-infected mice, when compared with uninfected controls, exhibited significant increase in EZH2 that co-localized with PCNA. Similarly, we observed increase in both membrane-bound and punctate nuclear staining for β -catenin that co-localized with EZH2 (Fig. 6B). We next isolated colonic crypts from CR-infected mice that were given Notch blocker DBZ for 10 days and grew them as colonoids. As shown in Fig. 6C, these colonoids appeared disintegrated with selective decrease in both EZH2/PCNA and EZH2/ β -catenin staining, respectively. Taken together, these findings underscore the relevance of infection-induced Wnt signaling in

the context of colonic crypt hyperplasia and how targeting these receptors may lead to early diagnosis and better outcome for colon cancer patients.

Before moving to the mechanistic studies, we next established the specificity of these changes *in vivo* by infecting NIH: Swiss mice with either WT or CR mutants, respectively. As shown in Fig. 7A, the levels of either LRP5 or LRP6 in *escV*-infected crypts were lower compared with levels in crypts from either WT or *espG*-infected mice. *escV* is a type 3 secretion system mutant that fails to inject CR's effector proteins into the host (16). The relative abundance of Fzd10 was also impacted by *escV*, but the reduction in levels was less obvious than those recorded for LRP5/6 (Fig. 7A). Pulldown assays in crypt (Fig. 7B, left) or CLP (Fig. 7B, right) with antibodies to either LRP5 or LRP6 followed by blotting with axin revealed axin's association with either protein at days 6–34 compared with uninfected controls. This led to increases in relative levels of β -catenin in response to CR infection at day 12 (Fig. 7C). These increases in β -catenin were attenuated in crypt extracts prepared from mice treated with Wnt inhibitor XAV939 (Fig. 7C) (31). We next utilized CT-26 cells to examine how the relative levels of these proteins changed in response to CR infection. As depicted in Fig. 7 (Di–Dv), relative increases in LRP5/6 and Fzd10 in response to CR infection coincided with increases in β -catenin. siRNA-induced knockdown of LRP5/6 or Fzd10 in CT-26 cells significantly reduced β -catenin/TCF-4-specific TOPflash reporter activity (Fig. 7E). These studies further validate infection-induced changes in Wnt receptors and how that impacts downstream Wnt signaling.

Because microRNA dysregulation and the Wnt/ β -catenin signaling have been implicated in driving the process of carcinogenesis, metastasis, and drug resistance, we next screened the NCCIT cells along with PA-1, HCT116, and HEK293 cells for differential regulation of miRNAs. As depicted in Fig. 8A, we detected varying levels of miR-221, miR-222, and miR-153-3p in the indicated cell lines. Of these miRNAs, miR-153-3p was consistently elevated in both NCCIT and PA-1 cells (Fig. 8A). These findings were corroborated in YAMC cells (Fig. S3A) and to some extent in CT-26 cells, particularly at 72 h after CR infection. Next, we used a plasmid-based miR inhibitor system (PMIS) (28) as a sponge to these miRNAs and performed a real-time PCR to examine the degree of inhibition. As depicted in Fig. 8B, PMIS-153- and PMIS-222-based sequestration led to a sharp decline in miR-153 and miR-222 levels, whereas PMIS-221 was less efficient. Next, we examined the effect of sequestering miR-153 on β -catenin/TCF-4-specific TOPflash reporter activity. As shown in Fig. 8C, the 3'-UTR of TCF-4 aligned perfectly with miR-153's seed sequence, and following PMIS-153-based sequestration, there was a uniform inhibition of the reporter activity across all of the indicated cell lines, sug-

Figure 1. Biochemical and molecular alterations in LRP5, LRP6, and Fzd10 dictate Wnt signaling and stemness *in vitro*. A, total RNAs isolated from HEK293, HCT116, NCCIT, and PA-1 cells were tested for the expression of LRP5, LRP6, Fzd10, and β -catenin through real-time quantitative PCR. Baseline expression profiles of the indicated markers are shown as box plots ($n \geq 3$ /group). B, Western blots showing the relative abundance of LRP5, LRP6, Fzd10, β -catenin, and EZH2 (Bi–Biii) along with the CSC markers ALDH1A1, *Dclk1*, and CD44 (Biv). Actin and H3 were used as loading controls, respectively ($n \geq 3$ /group). C, HEK293 and NCCIT cells were co-transfected with TOPflash reporter plasmid and siRNAs to LRP5 and LRP6 for 24 h, followed by measurement of reporter activity (p values as shown; $n \geq 3$ /group). D, NCCIT cells were transfected with either control siRNA or siRNAs to LRP5, LRP6, Fzd10, and EZH2 and grown in specific spheroid growth media in low adherent plates. After 1 week, spheroid formation was analyzed, and images were obtained with phase-contrast microscopy ($n \geq 3$ /group; scale bar, 50 μ m; $n = 5$ independent experiments). Error bars, S.D.



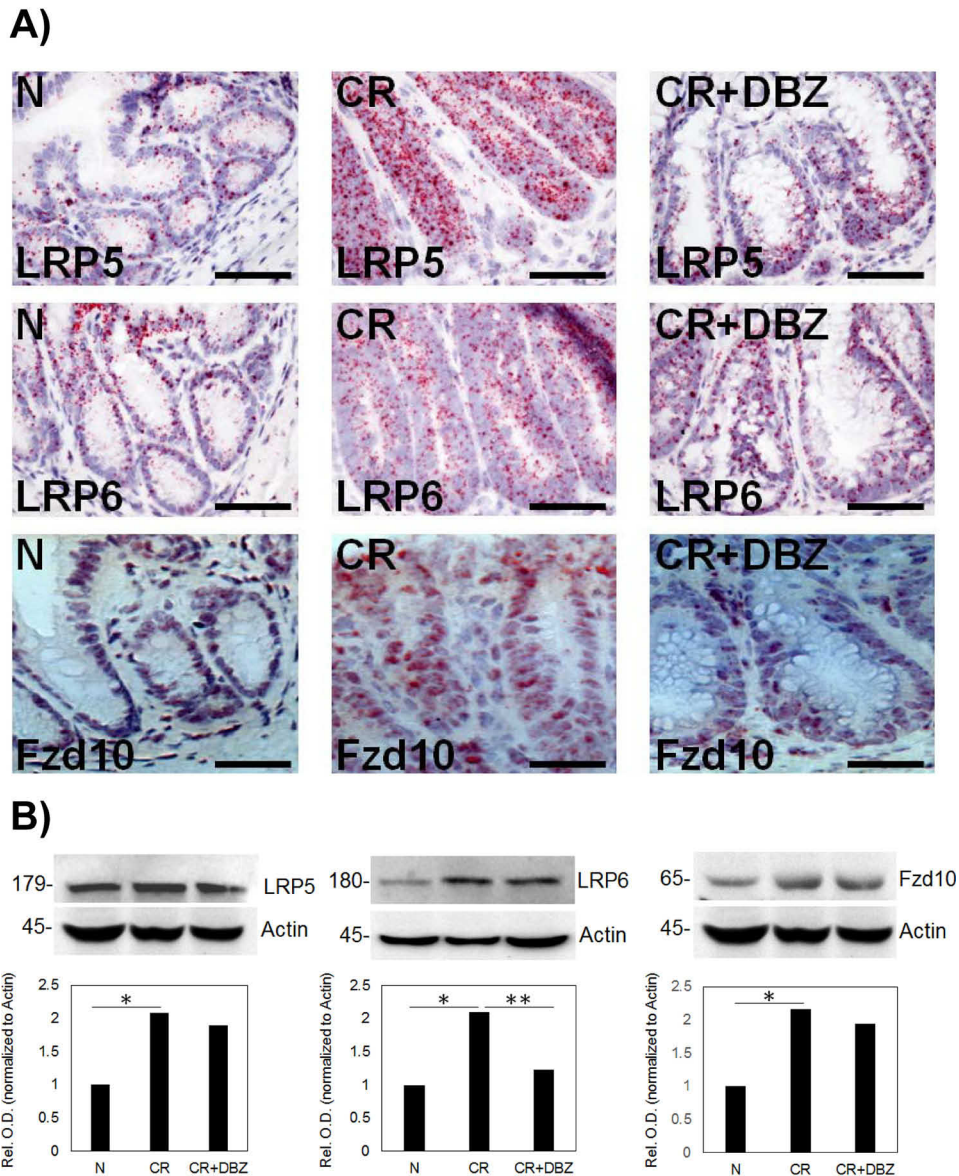


Figure 3. Cross-talk between Notch and Wnt pathway components. *A*, uninfected normal (*N*) NIH:Swiss mice were infected with CR and received the γ -secretase inhibitor DBZ (CR + DBZ) for 10 days, followed by euthanasia at day 12. Paraffin-embedded sections were analyzed by *in situ* hybridization. Bar, 150 μ m ($n \geq 5$ /group). *B*, *top*, total crypt extracts prepared from the group of mice described in *A* were probed with antibodies for LRP5, LRP6, and Fzd10. *Bottom*, bar graphs showing relative levels of LRP5/6 and Fzd10 normalized to actin. One-way ANOVA was used to examine statistical significance ($n \geq 3$ /group; *, $p < 0.05$ (*N* versus CR); **, $p < 0.05$ (CR versus CR + DBZ)).

gesting a positive role for miR-153-3p in Wnt signaling. A follow-up real-time PCR for the components of Wnt signaling impacted by the loss of miR-153-3p revealed significant down-regulation of Fzd10 with a less efficient decreases in LRP5 and LRP6, respectively (Fig. 8Di). Intriguingly, the seed sequence for miR-153-3p did not align with the Fzd10 3'-UTR (data not shown), suggesting an off-target effect. In contrast, we discovered down-regulation of Dclk1 levels following miR-153-3p loss and that Dclk1 3'-UTR aligned with miR-153-3p's seed sequence (Fig. 8Di). A follow-up Western blotting confirmed

decreases in Dclk1's relative abundance, whereas protein levels of other CSCs, including CD44 and ALDH1A1, were not affected (Fig. 8Dii). To determine whether reduction in Dclk1 levels influenced the growth of spheroids *in vitro*, we transfected NCCIT cells with either PMIS-153-3p or miRIDIAN-153 along with PMIS-221 followed by a spheroid assay. As shown in Fig. 8E and Fig. S4A, neither PMIS-153 or miRIDIAN-153 overexpression had any effect on spheroid growth. Similarly, PMIS-221 only marginally affected the spheroid growth. This lack of inhibitory effect on spheroid growth was further

Figure 2. *In situ* hybridization and protein levels of LRP5, LRP6, and Fzd10 correlate with ligand expression *in vivo*. *A*, *in situ* hybridization for LRP5, LRP6, and Fzd10 in the mouse distal colon tissue sections prepared at days 0 (*N*), 6 (*D6*), 12 (*D12*), 20 (*D20*), 27 (*D27*), and 34 (*D34*) after CR infection. *B*, total crypt (*B*) or CLP (*Bii*) extracts prepared from the group of mice described in *A* were probed with antibodies for LRP5, LRP6, and Fzd10. Actin was used as loading control ($n \geq 3$ /group; $n = 3$ independent experiments). *C*, RT-PCR of total RNA samples prepared from crypt or CLP isolated from the group of mice described in *A*. GAPDH was used as a loading control ($n \geq 3$ /group; $n = 3$ independent experiments).

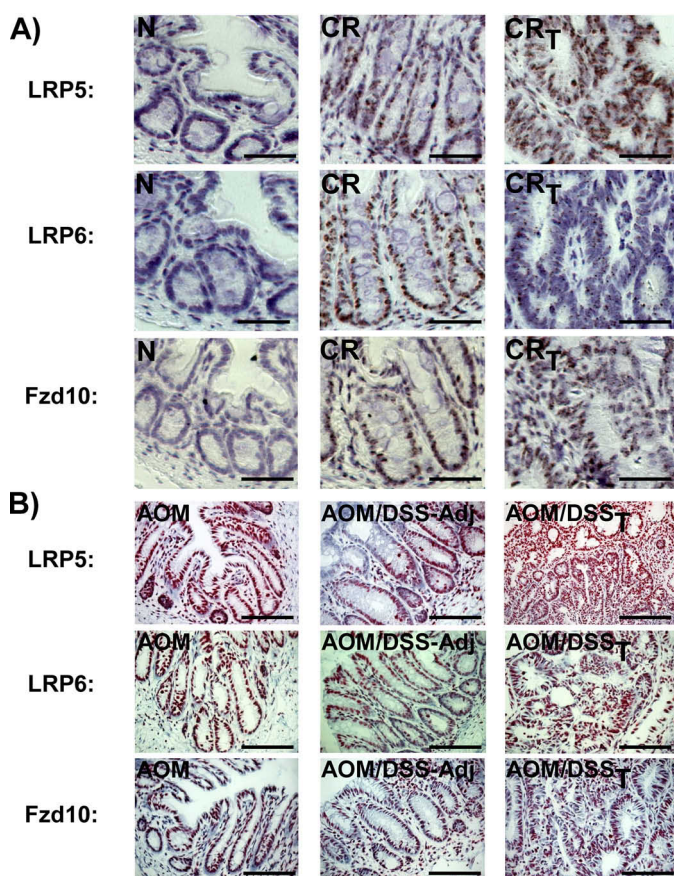


Figure 4. Colon tumors are endowed with higher levels of LRP5, LRP6 and Fzd10. *A*, representative photomicrographs of paraffin-embedded sections prepared from the distal colons of uninfected normal (N), CR-infected at day 12, or CR-infected *Apc*^{Min/+} mice at 3 months of age with tumor (CR_T). *In situ* hybridization was performed to detect changes in LRP5, LRP6, and Fzd10. Bar, 150 μm ($n \geq 3$ /group). *B*, paraffin-embedded sections prepared from AOM-treated or AOM + DSS-treated mice at 168 days were analyzed by *in situ* hybridization. Bar, 150 μm ($n \geq 3$ /group; $n = 3$ independent experiments).

confirmed following siRNA-induced knockdown of *Dcl1* (Fig. 8F). As proof-of-concept, we analyzed *Dcl1* promoter activities in the knocked down cells, and both long (*Dcl1*-L) and short (*Dcl1*-S) promoter activities were significantly inhibited in either HEK293 or NCCIT cells (Fig. S4B). Because levels of both CD44 and ALDH1A1 remained elevated after miR-153-3p sequestration, we also performed spheroid assays following siRNA-induced knockdown of CD44 and ALDH1A1, respectively. As revealed in Fig. 8 (G and H), only marginal inhibition of spheroid growth was observed, suggesting functional redundancies in CSCs that may require a multipronged approach for efficient targeting. We have shown previously that casein kinase-1 ϵ (CK1 ϵ) is up-regulated in response to CR infection (19). Because CK1 ϵ positively regulates Wnt signaling, which is key to CSC maintenance (29), we next measured CK1 ϵ expression in NCCIT and HEK293 cells following knockdown of *Dcl1*. As depicted in Fig. S4C, expression of CK1 ϵ in NCCIT cells with high endogenous Wnt signaling was mostly unchanged, whereas CK1 ϵ 's expression was significantly down-regulated in HEK293 cells after *Dcl1* knockdown, suggesting that CK1 ϵ may be fueling the spheroid growth in NCCIT cells knocked down for *Dcl1*. *In silico* binding studies indicated the

potential binding between Fzd10/Wnt2b (Fig. S5, A–C) and LRP6/Wnt2b (Fig. S5, D–F) as was revealed through molecular docking. Further examination revealed that WNT2B interacts with FZD10 and LRP6 through the same region but with different amino acids (Fig. S5, C and F). A similar binding pattern was obtained between LRP5/Wnt2b (data not shown). We further evaluated the predicted structures of Wnt2b and Fzd10 using the Ramachandran plot generated by PDBSUM (PROCHECK). Fig. S5 (G and H) represent the best and the most stable protein structure based on G-factor scores provided by PROCHECK. Fig. 9 is the schematic of possible mechanism of ligand-receptor engagement that transduces CR-induced Wnt signaling through β -catenin.

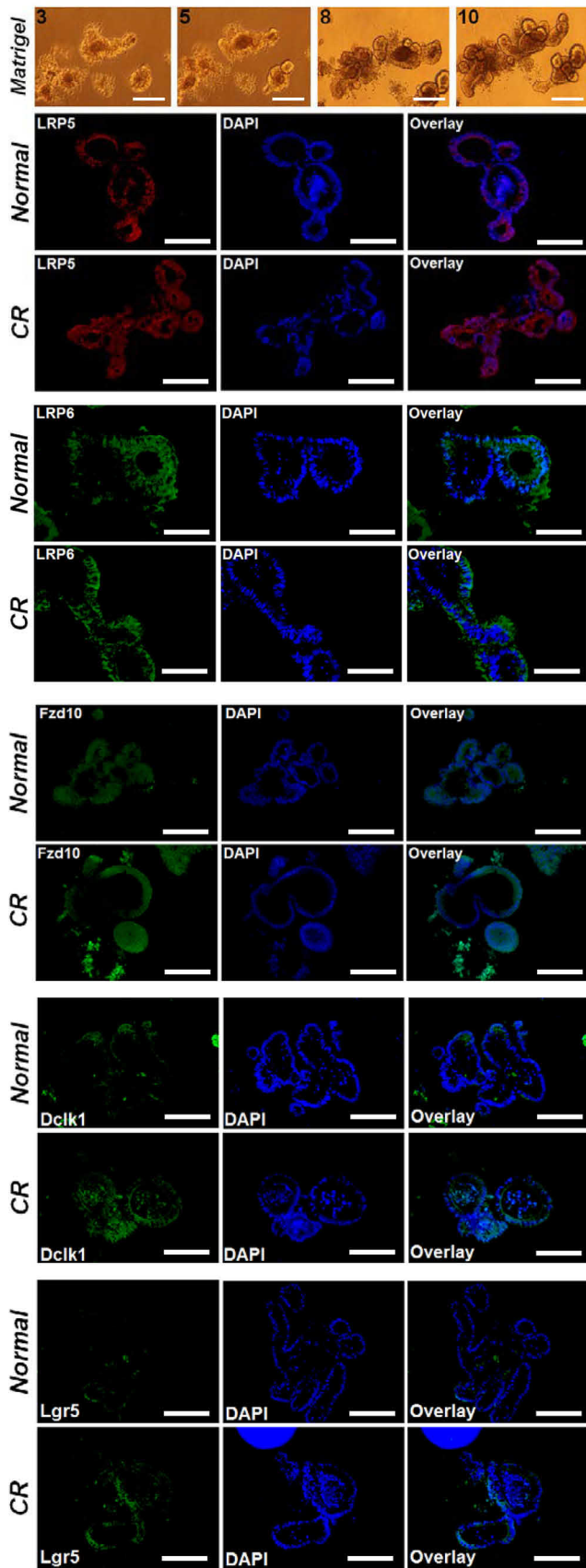
Discussion

Employing cell lines with elevated levels of endogenous Wnt signaling and a murine model of enteric infection, we elucidate the mechanism of epigenetic regulation of Wnt/ β -catenin signaling initiated at the plasma membrane and provide evidence that selective targeting of individual CSCs is not sufficient to block spheroid growth in an environment fueled by high Wnt signaling.

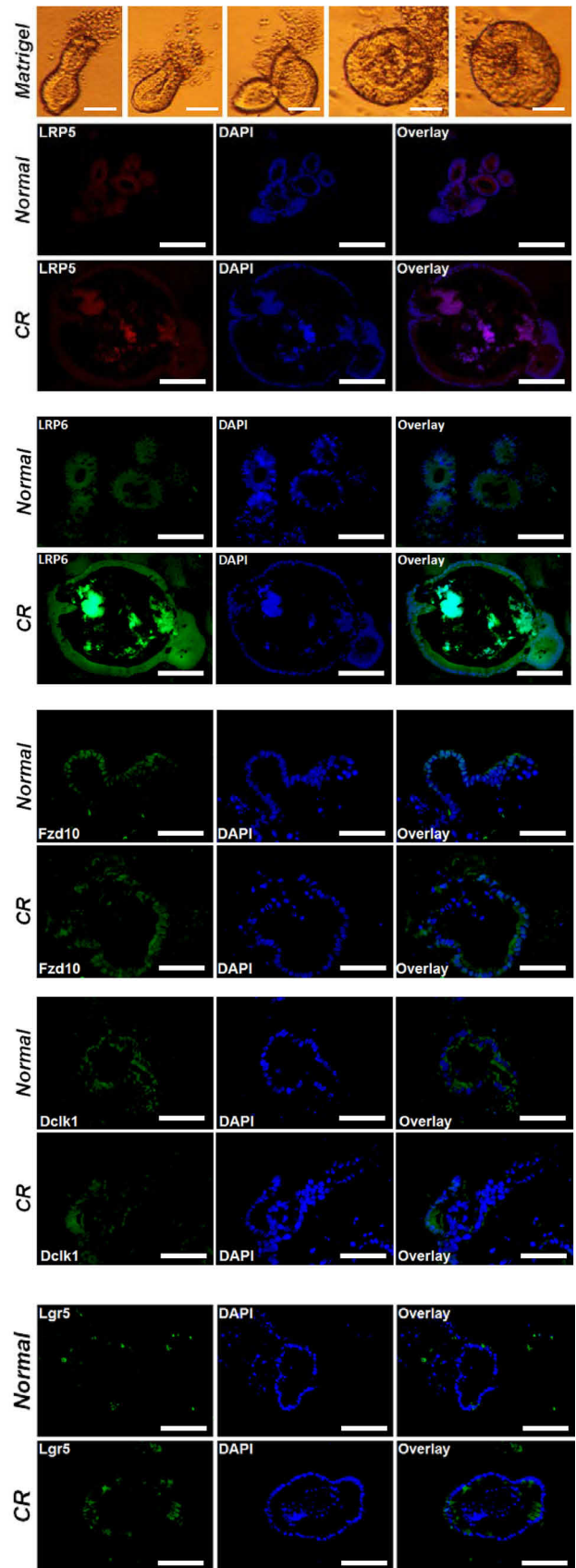
The canonical Wnt/ β -catenin pathway is activated when Wnt ligands bind to the Frizzled (FZD) receptors at the cell surface together with the low-density lipoprotein receptor-related protein (LRP) family receptors, LRP5/6. However, these membrane events are complicated and poorly elucidated, particularly in response to gastrointestinal infection. Certain pathogens harness Wnt-signaling components to promote infection. In one study, *Ehrlichia chaffeensis*, an obligate intracellular bacterium, was shown to utilize both β -catenin-dependent and -independent host Wnt signaling pathways to stimulate phagocytosis and promote intracellular survival (30). Similarly, *Chlamydia trachomatis*, a Gram-negative bacterium, was found to exploit Wnt/ β -catenin signaling to disturb epithelial tissue homeostasis in fallopian tubes (31). Despite these advances, the sequela of events that occur in response to infection, including the activation of LRP5/6 and FZD receptors that profoundly influence epithelial turnover within the gut, is poorly characterized. Using *in vitro* and *in vivo* approaches, we describe sequential changes in LRP5/6 and Fzd10 both at the mRNA and protein level in response to CR infection that coincides with β -catenin nuclear translocation and colonic crypt hyperplasia (19, 20, 24). In addition, we discovered a significant increase in canonical Wnt2b and noncanonical Wnt4 (32) ligand expression in the crypt that coincided with elevated LRP5/6 and Fzd10 expression, suggesting that they may be coordinating activation of these receptors to positively influence Wnt signaling in response to CR infection. Indeed, RT-PCR data in NCCIT cells transfected with siRNAs to Wnt2b showed a decline in Wnt2b expression coincident with decreases in TOPflash reporter activities. This is consistent with our previous findings, in which purified Wnt2b promoted β -catenin accumulation and β -catenin-dependent wound healing (33). Because CR infection causes infectious colitis in susceptible strains, these findings also align with Wnt pathway-related gene expression seen in inflammatory bowel disease (34).

Epigenetic regulation of Wnt signaling through enteric pathogen

A: Small Intestinal Organoids



B: Colon Organoids



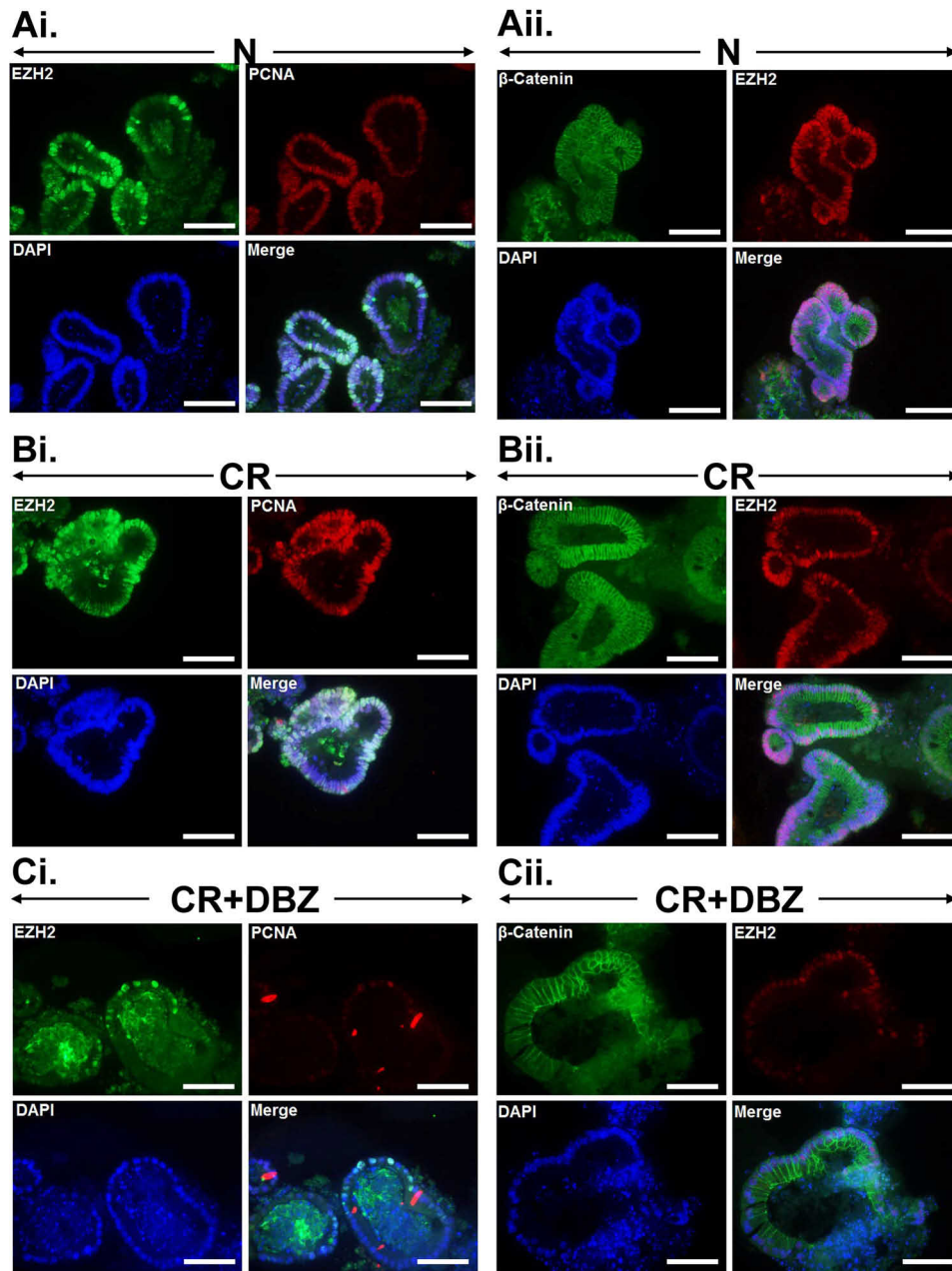


Figure 6. Infection-induced epigenetic changes underlie cross-talk between the Notch and the Wnt pathway. Colonic crypt cells isolated from uninfected normal (N) or CR-infected (CR) and CR-infected plus γ -secretase inhibitor DBZ-treated mice at day 12 were grown on Matrigel and co-stained with antibodies for EZH2 and PCNA or β -catenin and EZH2, respectively ($n \geq 3$ /group; scale bar, 50 μm ; $n = 3$ independent experiments). DAPI, 4',6-diamidino-2-phenylindole.

Notch and Wnt signals play essential roles in intestinal development and homeostasis. Ongoing and published studies employing a CR model have so far established that Wnt/ β -catenin, Notch, and phosphatidylinositol 3-kinase pathways regulate colonic crypt hyperplasia, whereas epithelial-stromal cross-talk, mediated by MEK/ERK/NF- κ B signaling, regulates inflammation and/or colitis in susceptible strains. We have also previously shown that CR infection regulates a functional cross-talk between Wnt/ β -catenin and Notch pathways and

that targeting the Notch pathway through the γ -secretase inhibitor DBZ also interferes with Wnt signaling, leading to inflammation and colitis (20). In the current study, we observed a significant decline in the levels of LRP5/6 and FZD10 in the colonic sections prepared from mice that received DBZ, suggesting the existence of a feedback loop that blocks elevated expression of these receptors in response to CR infection when the cross-talk no longer exists. In a similar study, it was shown previously that the proliferative effect of Notch signals requires

Figure 5. Infection-induced Wnt signaling promotes organoid growth *in vitro*. Small intestinal (A) or colon (B) crypt cells isolated from uninfected normal or CR-infected mice at day 12 were grown on Matrigel and stained with antibodies for LRP5, LRP6, Fzd10, Lgr5, and Dcl1, respectively ($n \geq 3$ /group; scale bars, 25 μm (bright field image) and 50 μm (immunostained spheroids); $n = 3$ independent experiments).

Epigenetic regulation of Wnt signaling through enteric pathogen

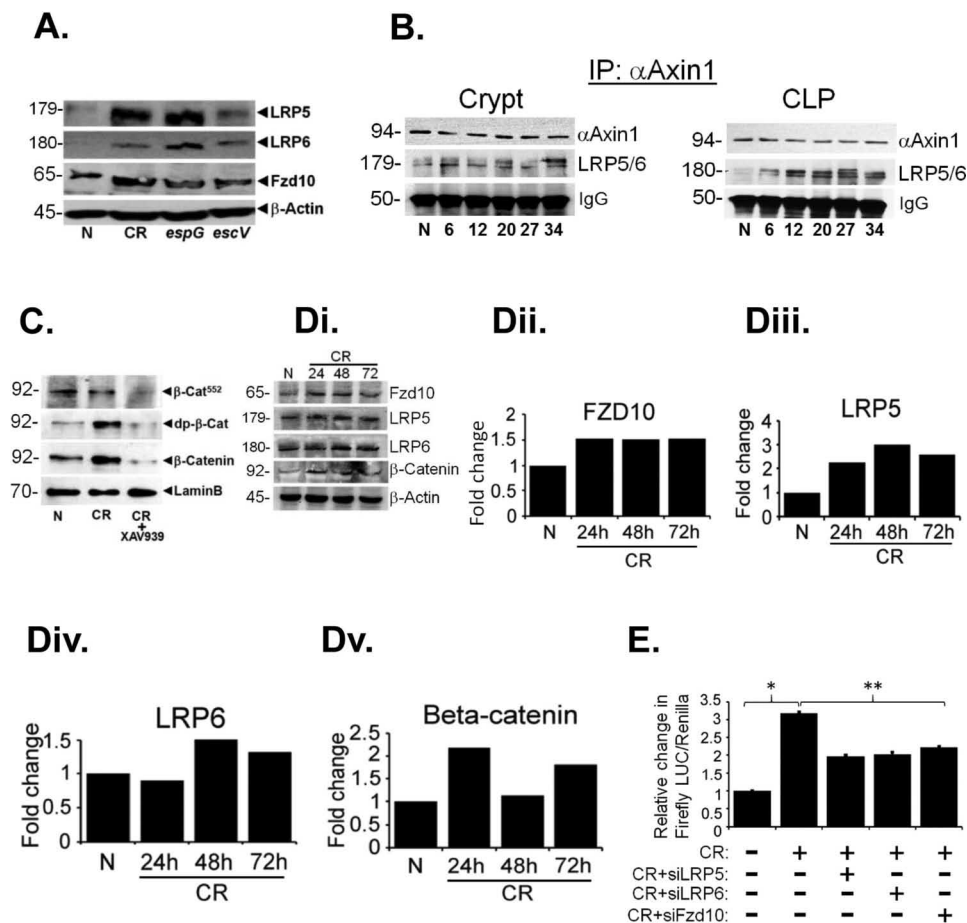
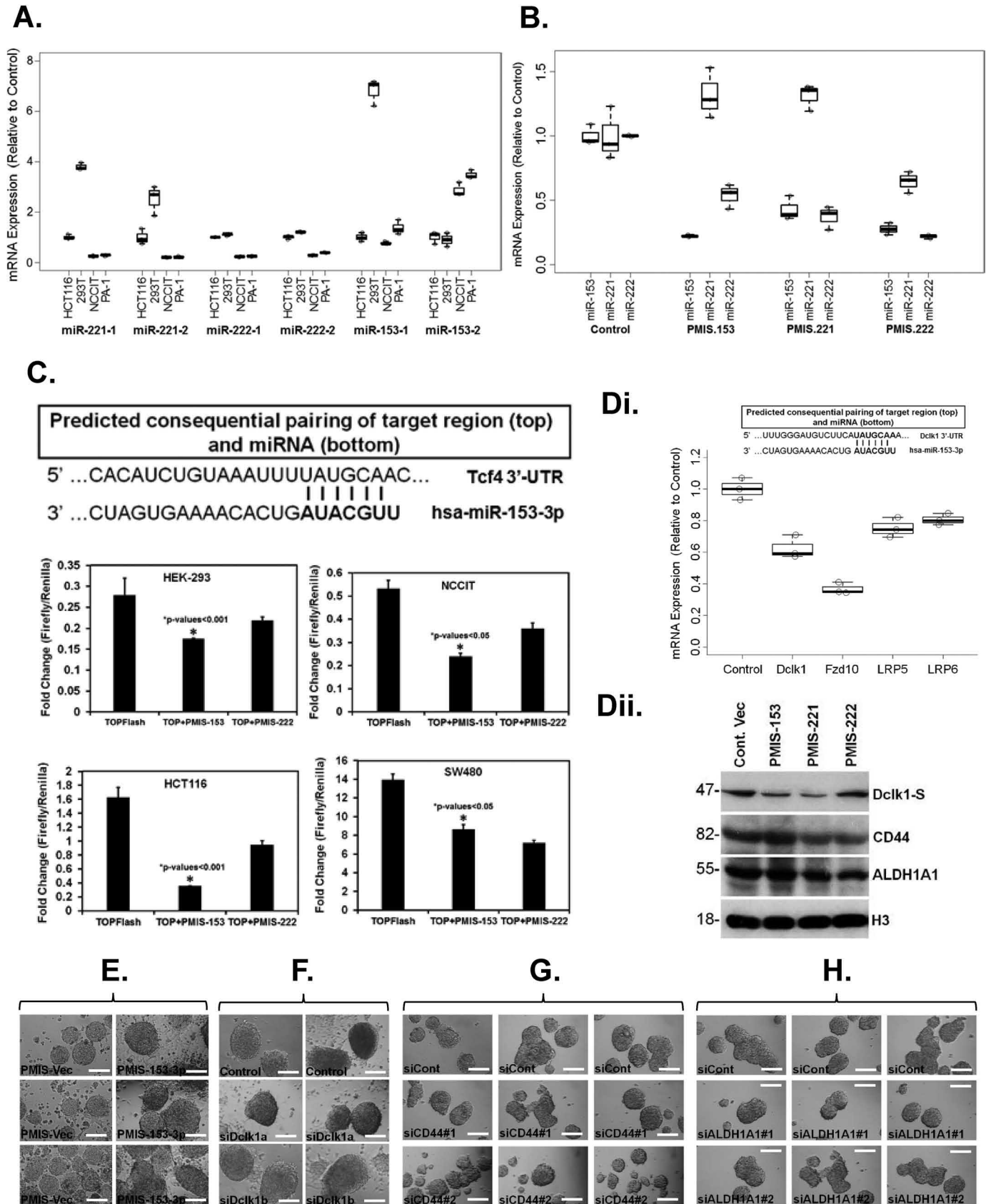


Figure 7. Specificity of changes in the components of the Wnt pathway *in vivo* and significance of abrogating Wnt signaling on wound healing *in vitro*. A, NIH:Swiss mice were either uninfected (N) or infected with WT CR or *espG* and *escV* mutants, respectively. Relative levels of LRP5, LRP6, and Fzd10 were determined in the colonic crypt extracts by Western blotting. Actin was used as loading control ($n \geq 3$ /group; $n = 3$ independent experiments). B, pull-down assays in the membrane fraction prepared from the colonic crypts (Bi) or crypt-denuded lamina propria (Bii) at days 0 (N), 6 (D6), 12 (D12), 20 (D20), 27 (D27), and 34 (D34) post-CR infection. Immunoprecipitation (IP) was performed with anti-axin-1 followed by blotting with either anti-axin-1 or LRP5, LRP6, and Fzd10. IgG heavy chain (IgG-H) was used as a loading control. C, NIH:Swiss mice were either uninfected (N) or infected with CR and CR + tankyrase inhibitor XAV939. Relative levels of active and total β -catenin were determined in the colonic crypt extracts by Western blotting. Lamin B was used as loading control ($n \geq 3$ /group; $n = 3$ independent experiments). D, WB showing relative abundance of Fzd10, LRP5, LRP6, and β -catenin in uninfected (N) or CR-infected CT-26 cells at 24, 48, or 72 h, respectively. Actin was used as a loading control. E, CT-26 cells were co-transfected with TOPflash reporter plasmid and siRNAs to LRP5, LRP6, and Fzd10 for 24 h, followed by measurement of reporter activity. One-way ANOVA was used to examine statistical significance ($n \geq 3$ /group; *, $p < 0.05$ (N versus CR); **, $p < 0.05$ (CR versus CR + siLRP5/6/Fzd10). Error bars, S.D.

normal Wnt signaling, whereas its influence on intestinal differentiation appears independent of Wnt (35). However, the synergy between these pathways has been shown to induce the formation of intestinal adenomas, particularly in the colon (35). We provide evidence of LRP5/6 or Fzd10 up-regulation in tumors isolated from the colons of either CR-infected *Apc^{Min/+}* or AOM/DSS-treated mice, respectively. This is consistent with a report in which Cripto-1, an EGF-Cripto-1/FRL1/Cryptic (CFC) gene family member (36), was shown to modulate the canonical Wnt/ β -catenin signaling pathway through direct interaction with the LRP5 and LRP6 co-receptors and was implicated in playing a role in mammary transformation (36). When we knocked down LRP5/6 and particularly Fzd10, there was significant increase in DICKKOPF-1 (DKK-1) mRNA expression. DICKKOPF-1 (DKK-1) encodes a secreted Wnt antagonist that binds to LRP5/6 and induces its endocytosis, leading to inhibition of the canonical pathway (37, 38). These results align with previous findings, in which González-Sancho *et al.* (39) described DKK-1 as a tumor suppressor gene, as its

loss led to development and progression of human colon cancer. The critical role of enteric pathogens in Wnt regulation has also been established using *Salmonella*, in which activation of Wnt/ β -catenin by *Salmonella* infection was shown to be associated with cell proliferation, inflammation, apoptosis, transdifferentiation, and tumorigenesis (40–48).

Colon cancer has been mainly viewed as a disease driven by the accumulation of genetic mutations. However, epigenetic mechanisms, including miRNAs, serve as vital players in modulating multiple biological processes, and dysregulation of oncogenic miRNAs induces constitutively active Wnt signaling in cancer (46). During screening of cell lines for miRNAs, we discovered significant changes in the expression and function of miR-153-3p. To associate miR-153-3p with Wnt signaling, we utilized a plasmid-based miRNA inhibition system (PMIS) pioneered by Brad Amendt's group (28) to show that PMIS-153-3p significantly blocked TOPflash reporter activity, suggesting that miR-153-3p positively regulates Wnt signaling. miR-153-3p is involved in the pathogenesis of acute graft-ver-



Epigenetic regulation of Wnt signaling through enteric pathogen

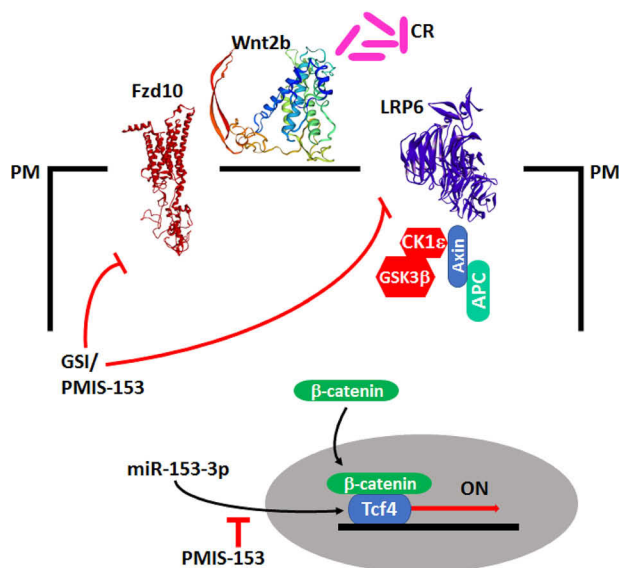


Figure 9. Schematic of proposed mechanism. We propose that in response to CR infection, Wnt2b interacts with both LRP5/6 (LRP6 shown as a prototypic example) and Fzd10 to promote β -catenin stabilization/nuclear translocation to positively impact Wnt signaling. Intervention via γ -secretase inhibitor (GSI) or miR-153-3p sequestration (PMIS153) can negatively impact Wnt signaling.

sus-host disease (47) and enhances cell radiosensitivity by targeting BCL2 in human glioma (48). In a recent study, it was shown that overexpression of miR-153 promoted β -catenin transcriptional activity, leading to cell-cycle progression, proliferation, and colony formation of hepatocellular carcinoma cells (49). We, however, provide the first evidence of miR-153-3p's regulation of Wnt signaling in colon cancer cells. Because aberrant activation of Wnt/ β -catenin signaling is associated with activation and maintenance of CSCs and miRNAs play a critical role in regulating CSC function, we evaluated the effect of PMIS-153 overexpression on CSCs. Unlike Dcl1, neither CD44 nor ALDH1A1 protein levels were affected by PMIS-153-3p. The 3'-UTR of Dcl1, however, aligned with the seed sequence in miR-153-3p that impacted Dcl1 levels. Encouraged by these results, we performed spheroid assays in cells transfected with PMIS-153 with the assumption that Dcl1 loss may influence spheroid growth. Contrary to our expectations, neither PMIS-153-3p overexpression nor siRNAs to Dcl1 affected spheroid growth in NCCIT cells that exhibit high endogenous Wnt signaling. Similarly, targeting CD44 or ALDH1A1 individually had only marginal impact on spheroid growth. It is important to highlight that not all CSCs express distinctive markers, and no marker set is exclusive to CSCs. Further complexity is attributed to change in marker profiles over time. Collectively, these findings underscore the heteroge-

neity among the CSCs and that a combinatorial approach may be needed to completely eradicate CSCs in an environment fueled by high Wnt signaling. Understanding the epigenetic regulation of human colorectal CSCs is expected to promote development of biomarkers for colorectal cancers and to identify targets for CSC-targeting therapies.

Experimental procedures

Murine model, treatments, and subcellular fractionation

Mouse housing, handling, and all of the related procedures were approved by the University of Kansas Medical Center Animal Care and Use Committee and were performed according to the Guide for the Care and Use of Laboratory Animals of the National Institutes of Health. Male *Helicobacter pylori*-free NIH:Swiss and *Apc*^{Min/+} mice at 5 and 6 weeks of age were procured from Jackson Laboratory (Bar Harbor, ME). NIH:Swiss or *Apc*^{Min/+} mice were infected by oral inoculation with a 16-h culture of either WT CR (biotype 4280, ATCC) or CR mutants espG and escV, respectively (at 10⁸ cfu) (50) identified as pink colonies on MacConkey agar, as described previously (16, 19–21, 24, 27, 51, 52). The escV mutant was constructed using SacB mutagenesis (50). Age- and sex-matched control mice received sterile culture medium only. To block the Notch pathway DBZ (EMD Chemicals, Inc., Gibbstown, NJ) suspensions was prepared as described elsewhere (20) and injected intraperitoneally in mice (at 10 μ mol/kg body weight) for 10 consecutive days beginning 2 days after CR infection (20, 53). For the AOM/DSS model following intraperitoneal pretreatment with azoxymethane (10 mg/kg body weight), the animals were subjected to three cycles of alternating administration of 2.5% DSS (36,000–50,000 molecular weight, SKU 0216011080, MP Biomedicals, Solon, OH) for 7 days followed by distilled water for 14 days. Mice were euthanized at 24 weeks after DSS treatment. Tankyrase-1/2 inhibition via XAV-939 was achieved through intraperitoneal injections at a dose of 1 mg/ml, once a day for 10 consecutive days (injection volume 100 μ l) based on previous publications (54). Control mice were injected with 100 μ l of XAV-939 solvent (10% DMSO, 90% of 0.9% NaCl). Total or nuclear fractions were prepared from colonic crypts isolated from uninfected mice or mice infected with CR for 6–34 days and stored at –80 °C until used for analyses.

Cell lines and plasmids

Unless mentioned otherwise, all cell lines were obtained from American Type Culture Collection (Manassas, VA). All cell lines were validated every 6 months or re-acquired from a new ATCC stock. In addition, all of the experiments were performed between the 5th and 20th passages. Cells were grown in 5% CO₂, Dulbecco's modified Eagle's medium, or RPMI con-

Figure 8. miRNAs and Wnt signaling. A, total RNAs isolated from HEK293, HCT116, NCCIT, and PA-1 cells were subjected to quantitative real-time RT-PCR (qRT-PCR) to examine expression of the indicated miRNAs ($n \geq 3$ /group). B, NCCIT cells were transfected with a PMIS specific to miR-153, miR-221, and miR-222. After 48 h, total RNA was isolated and subjected to qRT-PCR ($n \geq 3$ /group). C, NCCIT cells were co-transfected with TCF-4 reporter plasmid (TOPflash) or a mutant TCF-binding site (FOPflash), respectively, and pRL-TK *Renilla* vector was used as internal control. Twenty-four hours later, cells were transfected with either PMIS-153 or PMIS-222 for 24 h and analyzed by the Dual-Luciferase assay kit. The values were normalized to the internal control. *, $p < 0.001$ (HEK293 and HCT116) and $p < 0.05$ (NCCIT and SW480); $n = 3$ biological replicates). D, NCCIT cells were transfected with PMIS-153 or control vector for 24–48 h, and relative expression levels of LRP5, LRP6, Fzd10, and Dcl1 were determined either through qRT-PCR (Di; $n \geq 3$ /group) or Western blotting (Dii; $n \geq 3$ /group). E–H, NCCIT cells were transfected with either control vector or PMIS-153 (E), control siRNA or siRNAs to Dcl1 (F), CD44 (G), or ALDH1A1 (H) and grown in specific spheroid growth media in low adherent plates. After 1 week, spheroid formation was analyzed, and images were obtained with phase-contrast microscopy ($n \geq 3$ /group; scale bar, 25 μ m; $n = 5$ independent experiments). Error bars, S.D.

taining 10% fetal bovine serum and penicillin/streptomycin. YAMC and CT-26 cells were cultured as described elsewhere (27). All plasmid construct sequences were verified by automated DNA sequencing. PMIS vectors, including PMIS-miR-221, PMIS-miR-222, and PMIS-miR-153, were provided by NATUREmiRi (28) and validated in our laboratory.

Real-time and RT-PCR analyses

Total RNA was isolated from HEK293, HCT116, NCCIT, and PA-1 cells as well as from crypts or CLP at selected time points using TRIzolTM reagent. Expression levels of mRNA in the colonic crypts or CLP were measured by synthesis of cDNA from 2 μ g of total RNA via a high-capacity cDNA reverse transcription kit (Applied Biosystems, Foster City, CA). cDNAs were used for real-time PCR using Jumpstart TaqDNA polymerase (Sigma-Aldrich) and SYBR Green (Molecular Probes, Inc., Eugene, OR) nucleic acid stain as a marker for DNA amplification on a Bio-Rad CFX96 TouchTM real-time PCR detection system. Relative -fold change values were calculated with the comparative threshold cycle (ΔC_t) method normalized to GAPDH. Changes in mRNA expression were expressed as -fold change relative to control.

In situ hybridization

In situ hybridization analysis was performed on 4- μ m-thick formalin-fixed and paraffin-embedded colon tissue sections using the RNAscope 2.5 HD reagent kit-Brown/Red (Advanced Cell Diagnostics, Newark, CA), according to the manufacturer's instructions. In brief, the sections were deparaffinized, incubated with hydrogen peroxide for 10 min at room temperature, boiled with target retrieval for 15 min, and treated with protease at 40 °C for 30 min. The tissue sections were incubated with the desired probes (Designed by Advanced Cell Diagnostics) specific for LRP5, LRP6, and Fzd10 mRNA for 2 h at 40 °C. Incubations were done in the EZ Hybridization oven (ACD) using the humidity control tray (ACD). Signal amplification and detection steps were performed followed by counterstaining with hematoxylin. Sections were mounted using EcoMount (Biocare Medical), and pictures were taken with Nikon i80 microscope.

Immunoprecipitation and Western blotting

Total crypt cellular or nuclear extracts were prepared as described (16, 19–21, 27, 51). The isolated membrane extracts from the distal colons of uninfected control or day 6–34 CR-infected mice were precleared with 1 μ g of mouse IgG and 15 μ l of protein AG–agarose beads. The samples were immunoprecipitated with 2 μ g of axin-1 antibody overnight at 4 °C. Thereafter, 20 μ g of protein AG–agarose beads were added, and the samples were incubated for 45 min at 4 °C. The immunoprecipitates were washed multiple times with cold PBS. The precipitated protein samples were heated with 2 \times Laemmli sample buffer for 3 min and subjected to SDS-PAGE. Cell lysates from cell lines were prepared in radioimmunoprecipitation assay buffer with complete protease inhibitors (Roche Applied Science). Western blots were performed as described before (16, 19–21, 27, 51, 52).

Spheroid or organoid growth, wound-healing assays, and RNAi

Confluent monolayers of cells were trypsinized. Low cell-binding plates were used to seed the cells in corresponding culture medium containing 20 ng/ml fibroblast growth factor, 20 ng/ml epidermal growth factor (Sigma), and 10 ml/500 ml of B27 supplement (BD Biosciences) and cultured at 37 °C (5% CO₂, 100% humidity). Multicellular spheroids were designated as random spheroids and used for all experiments that employed larger populations of cells. Isolated crypts from uninfected or CR-infected and CR-infected plus DBZ-treated mouse distal colons were embedded in Matrigel for organoid culture according to the instructions in previous publications (16, 55–57). The siRNAs were purchased from Dharmacon (Lafayette, CO) or Fisher. Cells were transfected with 100 nM final concentrations of siRNA duplexes using Lipofectamine 2000 (Invitrogen), following the manufacturer's instructions. To determine luciferase reporter activity, TCF luciferase constructs (0.5 μ g), containing the WT (pTOPflash) or mutant (pFOPflash) (Upstate, Charlottesville, VA) TCF-binding sites along with an internal control (0.1 μ g of pRL-TK *Renilla* luciferase vector; Promega, Madison, WI) were transfected into NCCIT, HEK293, or CT26 cells (5×10^5 cells/well). Transfection experiments were carried out in triplicate using Lipofectamine 2000 (Invitrogen Life Technologies) following the manufacturer's instructions. The cells were incubated for 48 h and transfected with either PMIS (28) or siRNAs for 24 h followed by measurement of reporter activity using reagents from the Dual-Luciferase kit (Promega) as described previously (16).

Molecular docking

We used a molecular docking technique to study the interaction of Wnt2b with LRP6 and FFZD10. The LRP6 protein X-ray crystal structure was downloaded and extracted from the Protein Data Bank (entry 3S2K) (58). As Wnt2b and FZD10 have not been crystallized, we used a homology-modeling approach to generate their protein structures using the Swiss Model online program (<http://swissmodel.expasy.org/>) (59). SWISS-MODEL is a fully automated server for protein structure prediction using homology modeling. It is accessible via the ExpASY web server or from the program DeepView, also known as Swiss PDB Viewer. The predicted structures were evaluated by using the Ramachandran plot generated by PDBSUM (PROCHECK), and the most stable protein structure was selected based on *G*-factor scores. The protein-protein modeling was performed by using the GRAMM-X Protein-Protein Docking web server (60). The best stable predicted interaction was selected and visualized using Discovery studio.

Statistical analysis

Statistical analyses were performed using both parametric and nonparametric tests; the latter is robust to departures from normality and was used in cases where sample sizes involved in the comparisons were limited. Specifically, unpaired, two-tailed Student's *t* tests and Wilcoxon rank-sum tests were used for two-group comparisons. One-way analysis of variance

Epigenetic regulation of Wnt signaling through enteric pathogen

(ANOVA) models were used for multiple-group comparisons (GraphPad Prism version 5). $p < 0.05$ was considered statistically significant.

Author contributions—I. A., B. C. R., and S. U. data curation; I. A., B. C. R., L. U. M. R. J., and S. U. formal analysis; I. A., B. C. R., S. A., V. S., and S. U. validation; I. A., B. C. R., L. U. M. R. J., D. S., and S. U. investigation; I. A., B. C. R., V. S., and S. U. visualization; I. A., B. C. R., L. U. M. R. J., and D. S. methodology; I. A. writing-review and editing; P. D., S. A., V. S., and S. U. software; S. A., V. S., and S. U. resources; S. A. and S. U. supervision; S. U. conceptualization; S. U. funding acquisition; S. U. writing-original draft; S. U. project administration.

References

- Clevers, H., and Nusse, R. (2012) Wnt/ β -catenin signaling and disease. *Cell* **149**, 1192–1205 [CrossRef Medline](#)
- Nishisho, I., Nakamura, Y., Miyoshi, Y., Miki, Y., Ando, H., Horii, A., Koyama, K., Utsunomiya, J., Baba, S., and Hedge, P. (1991) Mutations of chromosome 5q21 genes in FAP and colorectal cancer patients. *Science* **253**, 665–669 [CrossRef Medline](#)
- MacDonald, B. T., and He, X. (2012) Frizzled and LRP5/6 receptors for Wnt/ β -catenin signaling. *Cold Spring Harb. Perspect. Biol.* **4**, a007880 [CrossRef Medline](#)
- Cancer Genome Atlas Network (2012) Comprehensive molecular characterization of human colon and rectal cancer. *Nature* **487**, 330–337 [CrossRef Medline](#)
- Giannakis, M., Hodis, E., Jasmine Mu, X., Yamauchi, M., Rosenbluh, J., Cibulskis, K., Saksena, G., Lawrence, M. S., Qian, Z. R., Nishihara, R., Van Allen, E. M., Hahn, W. C., Gabriel, S. B., Lander, E. S., Getz, G., et al. (2014) RNF43 is frequently mutated in colorectal and endometrial cancers. *Nat. Genet.* **46**, 1264–1266 [CrossRef Medline](#)
- Morin, P. J., Sparks, A. B., Korinek, V., Barker, N., Clevers, H., Vogelstein, B., and Kinzler, K. W. (1997) Activation of β -catenin-Tcf signaling in colon cancer by mutations in β -catenin or APC. *Science* **275**, 1787–1790 [CrossRef Medline](#)
- Holmen, S. L., Giambernardi, T. A., Zylstra, C. R., Buckner-Berghuis, B. D., Resau, J. H., Hess, J. F., Glatt, V., Bouxsein, M. L., Ai, M., Warman, M. L., and Williams, B. O. (2004) Decreased BMD and limb deformities in mice carrying mutations in both Lrp5 and Lrp6. *J. Bone Miner. Res.* **19**, 2033–2040 [CrossRef Medline](#)
- Kelly, O. G., Pinson, K. I., and Skarnes, W. C. (2004) The Wnt co-receptors Lrp5 and Lrp6 are essential for gastrulation in mice. *Development* **131**, 2803–2815 [CrossRef Medline](#)
- de Voer, R. M., Hahn, M. M., Weren, R. D., Mensenkamp, A. R., Gilissen, C., van Zelst-Stams, W. A., Spruijt, L., Kets, C. M., Zhang, J., Venselaar, H., Vreede, L., Schubert, N., Tychon, M., Derks, R., Schackert, H. K., et al. (2016) Identification of novel candidate genes for early-onset colorectal cancer susceptibility. *PLoS Genet.* **12**, e1005880 [CrossRef Medline](#)
- Shimokawa, M., Ohta, Y., Nishikori, S., Matano, M., Takano, A., Fujii, M., Date, S., Sugimoto, S., Kanai, T., and Sato, T. (2017) Visualization and targeting of LGR5⁺ human colon cancer stem cells. *Nature* **545**, 187–192 [CrossRef Medline](#)
- Munro, M. J., Wickremesekera, S. K., Peng, L., Tan, S. T., and Itinteang, T. (2018) Cancer stem cells in colorectal cancer: a review. *J. Clin. Pathol.* **71**, 110–116 [CrossRef Medline](#)
- Ricci-Vitiani, L., Fabrizi, E., Palio, E., and De Maria, R. (2009) Colon cancer stem cells. *J. Mol. Med.* **87**, 1097–1104 [CrossRef Medline](#)
- Merlos-Suárez, A., Barriga, F. M., Jung, P., Iglesias, M., Céspedes, M. V., Rossell, D., Sevillano, M., Hernando-Mombalona, X., da Silva-Diz, V., Muñoz, P., Clevers, H., Sancho, E., Mangués, R., and Batlle, E. (2011) The intestinal stem cell signature identifies colorectal cancer stem cells and predicts disease relapse. *Cell Stem Cell* **8**, 511–524 [CrossRef Medline](#)
- Nakanishi, Y., Seno, H., Fukuoka, A., Ueo, T., Yamaga, Y., Maruno, T., Nakanishi, N., Kanda, K., Komekado, H., Kawada, M., Isomura, A., Kawada, K., Sakai, Y., Yanagita, M., Kageyama, R., et al. (2013) Dcl1 distinguishes between tumor and normal stem cells in the intestine. *Nat. Genet.* **45**, 98–103 [CrossRef Medline](#)
- Mens, M. M. J., and Ghanbari, M. (2018) Cell cycle regulation of stem cells by microRNAs. *Stem Cell Rev. Rep.* **14**, 309–322 [CrossRef Medline](#)
- Roy, B. C., Subramaniam, D., Ahmed, I., Jala, V. R., Hester, C. M., Greiner, K. A., Haribabu, B., Anant, S., and Umar, S. (2015) Role of bacterial infection in the epigenetic regulation of Wnt antagonist WIF1 by PRC2 protein EZH2. *Oncogene* **34**, 4519–4530 [CrossRef Medline](#)
- Collins, J. W., Keeney, K. M., Crepin, V. F., Rathinam, V. A., Fitzgerald, K. A., Finlay, B. B., and Frankel, G. (2014) *Citrobacter rodentium*: infection, inflammation and the microbiota. *Nat. Rev. Microbiol.* **12**, 612–623 [CrossRef Medline](#)
- Mundy, R., MacDonald, T. T., Dougan, G., Frankel, G., and Wiles, S. (2005) *Citrobacter rodentium* of mice and man. *Cell Microbiol.* **7**, 1697–1706 [CrossRef Medline](#)
- Umar, S., Wang, Y., Morris, A. P., and Sellin, J. H. (2007) Dual alterations in casein kinase I-epsilon and GSK-3 β modulate β -catenin stability in hyperproliferating colonic epithelia. *Am. J. Physiol. Gastrointest. Liver Physiol.* **292**, G599–G607 [CrossRef Medline](#)
- Ahmed, I., Chandrakesan, P., Tawfik, O., Xia, L., Anant, S., and Umar, S. (2012) Critical roles of Notch and Wnt/ β -catenin pathways in the regulation of hyperplasia and/or colitis in response to bacterial infection. *Infect. Immun.* **80**, 3107–3121 [CrossRef Medline](#)
- Ahmed, I., Roy, B., Chandrakesan, P., Venugopal, A., Xia, L., Jensen, R., Anant, S., and Umar, S. (2013) Evidence of functional cross talk between the Notch and NF- κ B pathways in nonneoplastic hyperproliferating colonic epithelium. *Am. J. Physiol. Gastrointest. Liver Physiol.* **304**, G356–G370 [CrossRef Medline](#)
- Ye, Z., Petrof, E. O., Boone, D., Claud, E. C., and Sun, J. (2007) *Salmonella* effector AvrA regulation of colonic epithelial cell inflammation by deubiquitination. *Am. J. Pathol.* **171**, 882–892 [CrossRef Medline](#)
- Hemmati, H. D., Nakano, I., Lazareff, J. A., Masterman-Smith, M., Geschwind, D. H., Bronner-Fraser, M., and Kornblum, H. I. (2003) Cancerous stem cells can arise from pediatric brain tumors. *Proc. Natl. Acad. Sci. U.S.A.* **100**, 15178–15183 [CrossRef Medline](#)
- Sellin, J. H., Wang, Y., Singh, P., and Umar, S. (2009) β -Catenin stabilization imparts crypt progenitor phenotype to hyperproliferating colonic epithelia. *Exp. Cell Res.* **315**, 97–109 [CrossRef Medline](#)
- Newman, J. V., Kosaka, T., Sheppard, B. J., Fox, J. G., and Schauer, D. B. (2001) Bacterial infection promotes colon tumorigenesis in *Apc*^{Min/+} mice. *J. Infect. Dis.* **184**, 227–230 [CrossRef Medline](#)
- Barrila, J., Crabbe, A., Yang, J., Franco, K., Nydam, S. D., Forsyth, R. J., Davis, R. R., Gangaraju, S., Ott, C. M., Coyne, C. B., Bissell, M. J., and Nickerson, C. A. (2018) Modeling host-pathogen interactions in the context of the microenvironment: three-dimensional cell culture comes of age. *Infect. Immun.* **86**, e00282-18 [CrossRef Medline](#)
- Chandrakesan, P., Roy, B., Jakkula, L. U., Ahmed, I., Ramamoorthy, P., Tawfik, O., Papineni, R., Houchen, C., Anant, S., and Umar, S. (2014) Utility of a bacterial infection model to study epithelial-mesenchymal transition, mesenchymal-epithelial transition or tumorigenesis. *Oncogene* **33**, 2639–2654 [CrossRef Medline](#)
- Cao, H., Yu, W., Li, X., Wang, J., Gao, S., Holton, N. E., Eliason, S., Sharp, T., and Amendt, B. A. (2016) A new plasmid-based microRNA inhibitor system that inhibits microRNA families in transgenic mice and cells: a potential new therapeutic reagent. *Gene Ther.* **23**, 527–542 [CrossRef Medline](#)
- Morgenstern, Y., Das Adhikari, U., Ayyash, M., Elyada, E., Tóth, B., Moor, A., Itzkovitz, S., and Ben-Neriah, Y. (2017) Casein kinase 1- ϵ or 1- δ required for Wnt-mediated intestinal stem cell maintenance. *EMBO J.* **36**, 3046–3061 [CrossRef Medline](#)
- Luo, T., Dunphy, P. S., Lina, T. T., and McBride, J. W. (2015) *Ehrlichia chaffeensis* exploits canonical and noncanonical host Wnt signaling pathways to stimulate phagocytosis and promote intracellular survival. *Infect. Immun.* **84**, 686–700 [CrossRef Medline](#)
- Kessler, M., Zielecki, J., Thieck, O., Mollenkopf, H. J., Fotopoulou, C., and Meyer, T. F. (2012) *Chlamydia trachomatis* disturbs epithelial tissue ho-

- meostasis in fallopian tubes via paracrine Wnt signaling. *Am. J. Pathol.* **180**, 186–198 [CrossRef Medline](#)
32. Ring, L., Neth, P., Weber, C., Steffens, S., and Faussner, A. (2014) β -Catenin-dependent pathway activation by both promiscuous “canonical” WNT3a-, and specific “noncanonical” WNT4- and WNT5a-FZD receptor combinations with strong differences in LRP5 and LRP6 dependency. *Cell. Signal.* **26**, 260–267 [CrossRef Medline](#)
 33. Chandrakesan, P., Jakkula, L. U., Ahmed, I., Roy, B., Anant, S., and Umar, S. (2013) Differential effects of β -catenin and NF- κ B interplay in the regulation of cell proliferation, inflammation and tumorigenesis in response to bacterial infection. *PLoS One* **8**, e79432 [CrossRef Medline](#)
 34. You, J., Nguyen, A. V., Albers, C. G., Lin, F., and Holcombe, R. F. (2008) Wnt pathway-related gene expression in inflammatory bowel disease. *Dig. Dis. Sci.* **53**, 1013–1019 [CrossRef Medline](#)
 35. Fre, S., Pallavi, S. K., Huyghe, M., Laé, M., Janssen, K. P., Robine, S., Artavanis-Tsakonas, S., and Louvard, D. (2009) Notch and Wnt signals cooperatively control cell proliferation and tumorigenesis in the intestine. *Proc. Natl. Acad. Sci. U.S.A.* **106**, 6309–6314 [CrossRef Medline](#)
 36. Nagaoka, T., Karasawa, H., Turbyville, T., Rangel, M. C., Castro, N. P., Gonzales, M., Baker, A., Seno, M., Lockett, S., Greer, Y. E., Rubin, J. S., Salomon, D. S., and Bianco, C. (2013) Cripto-1 enhances the canonical Wnt/ β -catenin signaling pathway by binding to LRP5 and LRP6 co-receptors. *Cell. Signal.* **25**, 178–189 [CrossRef Medline](#)
 37. Zorn, A. M. (2001) Wnt signalling: antagonistic Dickkopfs. *Curr. Biol.* **11**, R592–R595 [CrossRef Medline](#)
 38. Kawano, Y., and Kypta, R. (2003) Secreted antagonists of the Wnt signaling pathway. *J. Cell Sci.* **116**, 2627–2634 [CrossRef Medline](#)
 39. González-Sancho, J. M., Aguilera, O., García, J. M., Pendás-Franco, N., Peña, C., Cal, S., García de Herreros, A., Bonilla, F., and Muñoz, A. (2005) The Wnt antagonist DICKKOPF-1 gene is a downstream target of β -catenin/TCF and is downregulated in human colon cancer. *Oncogene* **24**, 1098–1103 [CrossRef Medline](#)
 40. Sun, J., Hobert, M. E., Rao, A. S., Neish, A. S., and Madara, J. L. (2004) Bacterial activation of β -catenin signaling in human epithelia. *Am. J. Physiol. Gastrointest. Liver Physiol.* **287**, G220–G227 [CrossRef Medline](#)
 41. Tahoun, A., Mahajan, S., Paxton, E., Malterer, G., Donaldson, D. S., Wang, D., Tan, A., Gillespie, T. L., O’Shea, M., Roe, A. J., Shaw, D. J., Gally, D. L., Lengeling, A., Mabbott, N. A., Haas, J., and Mahajan, A. (2012) *Salmonella* transforms follicle-associated epithelial cells into M cells to promote intestinal invasion. *Cell Host Microbe* **12**, 645–656 [CrossRef Medline](#)
 42. Lu, R., Liu, X., Wu, S., Xia, Y., Zhang, Y. G., Petrof, E. O., Claud, E. C., and Sun, J. (2012) Consistent activation of the β -catenin pathway by *Salmonella* type-three secretion effector protein AvrA in chronically infected intestine. *Am. J. Physiol. Gastrointest. Liver Physiol.* **303**, G1113–G1125 [CrossRef Medline](#)
 43. Liu, X., Lu, R., Wu, S., and Sun, J. (2010) *Salmonella* regulation of intestinal stem cells through the Wnt/ β -catenin pathway. *FEBS Lett.* **584**, 911–916 [CrossRef Medline](#)
 44. Liu, X., Wu, S., Xia, Y., Li, X. E., Xia, Y., Zhou, Z. D., and Sun, J. (2011) Wingless homolog Wnt11 suppresses bacterial invasion and inflammation in intestinal epithelial cells. *Am. J. Physiol. Gastrointest. Liver Physiol.* **301**, G992–G1003 [CrossRef Medline](#)
 45. Mughini-Gras, L., Schaapveld, M., Kramers, J., Mooij, S., Neeffes-Borst, E. A., Pelt, W. V., and Neeffes, J. (2018) Increased colon cancer risk after severe *Salmonella* infection. *PLoS One* **13**, e0189721 [CrossRef Medline](#)
 46. You, J. S., and Jones, P. A. (2012) Cancer genetics and epigenetics: two sides of the same coin? *Cancer Cell* **22**, 9–20 [CrossRef Medline](#)
 47. Zhao, X. S., Wang, Y. N., Lv, M., Kong, Y., Luo, H. X., Ye, X. Y., Wu, Q., Zhao, T. F., Hu, Y. H., Zhang, H. Y., Huo, M. R., Wan, J., and Huang, X. J. (2016) miR-153-3p, a new bio-target, is involved in the pathogenesis of acute graft-versus-host disease via inhibition of indoleamine-2,3-dioxygenase. *Oncotarget* **7**, 48321–48334 [CrossRef Medline](#)
 48. Sun, D., Mu, Y., and Piao, H. (2018) MicroRNA-153-3p enhances cell radiosensitivity by targeting BCL2 in human glioma. *Biol. Res.* **51**, 56 [CrossRef Medline](#)
 49. Hua, H. W., Jiang, F., Huang, Q., Liao, Z., and Ding, G. (2015) MicroRNA-153 promotes Wnt/ β -catenin activation in hepatocellular carcinoma through suppression of WWOX. *Oncotarget* **6**, 3840–3847 [CrossRef Medline](#)
 50. Hardwidge, P. R., Deng, W., Vallance, B. A., Rodriguez-Escudero, I., Cid, V. J., Molina, M., and Finlay, B. B. (2005) Modulation of host cytoskeleton function by the enteropathogenic *Escherichia coli* and *Citrobacter rodentium* effector protein EspG. *Infect. Immun.* **73**, 2586–2594 [CrossRef Medline](#)
 51. Chandrakesan, P., Ahmed, I., Chinthapally, A., Singh, P., Awasthi, S., Anant, S., and Umar, S. (2012) Distinct compartmentalization of NF- κ B activity in crypt and crypt-denuded lamina propria precedes and accompanies hyperplasia and/or colitis following bacterial infection. *Infect. Immun.* **80**, 753–767 [CrossRef Medline](#)
 52. Chandrakesan, P., Ahmed, I., Anwar, T., Wang, Y., Sarkar, S., Singh, P., Peleg, S., and Umar, S. (2010) Novel changes in NF- κ B activity during progression and regression phases of hyperplasia: role of MEK, ERK, and p38. *J. Biol. Chem.* **285**, 33485–33498 [CrossRef Medline](#)
 53. Milano, J., McKay, J., Dagenais, C., Foster-Brown, L., Pognan, F., Gadiant, R., Jacobs, R. T., Zacco, A., Greenberg, B., and Ciaccio, P. J. (2004) Modulation of notch processing by γ -secretase inhibitors causes intestinal goblet cell metaplasia and induction of genes known to specify gut secretory lineage differentiation. *Toxicol. Sci.* **82**, 341–358 [CrossRef Medline](#)
 54. Bai, J., Liu, Z., Xu, Z., Ke, F., Zhang, L., Zhu, H., Lou, F., Wang, H., Fei, Y., Shi, Y. L., and Wang, H. (2015) Epigenetic downregulation of SFRP4 contributes to epidermal hyperplasia in psoriasis. *J. Immunol.* **194**, 4185–4198 [CrossRef Medline](#)
 55. Wang, Y., Ahmad, A. A., Shah, P. K., Sims, C. E., Magness, S. T., and Allbritton, N. L. (2013) Capture and 3D culture of colonic crypts and colonoids in a microarray platform. *Lab Chip* **13**, 4625–4634 [CrossRef Medline](#)
 56. Sato, T., Stange, D. E., Ferrante, M., Vries, R. G., Van Es, J. H., Van den Brink, S., Van Houdt, W. J., Pronk, A., Van Gorp, J., Siersema, P. D., and Clevers, H. (2011) Long-term expansion of epithelial organoids from human colon, adenoma, adenocarcinoma, and Barrett’s epithelium. *Gastroenterology* **141**, 1762–1772 [CrossRef Medline](#)
 57. Miyoshi, H., and Stappenbeck, T. S. (2013) *In vitro* expansion and genetic modification of gastrointestinal stem cells in spheroid culture. *Nat. Protoc.* **8**, 2471–2482 [CrossRef Medline](#)
 58. Ahn, V. E., Chu, M. L., Choi, H. J., Tran, D., Abo, A., and Weis, W. I. (2011) Structural basis of Wnt signaling inhibition by Dickkopf binding to LRP5/6. *Dev. Cell* **21**, 862–873 [CrossRef Medline](#)
 59. Waterhouse, A., Bertoni, M., Bienert, S., Studer, G., Tauriello, G., Gumienny, R., Heer, F. T., de Beer, T. A. P., Rempfer, C., Bordoli, L., Lepore, R., and Schwede, T. (2018) SWISS-MODEL: homology modelling of protein structures and complexes. *Nucleic Acids Res.* **46**, W296–W303 [CrossRef Medline](#)
 60. Tovchigrechko, A., and Vakser, I. A. (2006) GRAMM-X public web server for protein-protein docking. *Nucleic Acids Res.* **34**, W310–W314 [CrossRef Medline](#)